5146 *Macromolecules* **2009**, *42*, 5146–5154
DOI: 10.1021/ma900703j

Macromolecules
ARTICLE

Nanostructured Proton Conducting Polystyrene−Poly(vinylphosphonic acid) Block Copolymers Prepared via Sequential Anionic Polymerizations

Renaud Perrin,[†] Matti Elomaa,[‡] and Patric Jannasch*,[†]

[†]*Department of Chemistry, Polymer & Materials Chemistry, Lund University, P.O. Box 124, SE-221 00 Lund, Sweden, and* [‡]*Laboratory of Polymer Chemistry, PB 55, 00014 University of Helsinki, Finland*

Received April 1, 2009; Revised Manuscript Received May 14, 2009

ABSTRACT: Poly(styrene-*b*-vinylphosphonic acid) diblock copolymers have been prepared via sequential anionic polymerization and evaluated as nanostructured polymer electrolytes. The ionic block copolymers were synthesized by first initiating the polymerization of styrene using *n*-butyllithium in tetrahydrofuran at −78 °C. 1,1-Diphenylethylene was then added to the living polystyryl anions before charging diethyl vinylphosphonate to polymerize the second block. The poly(diethyl phosphonate) block was subsequently completely hydrolyzed to obtain the poly(vinylphosphonic acid) block. Analysis by calorimetry showed two distinct glass transitions of the acidic copolymers, indicating phase separation between the two blocks. The glass transition temperature of the densely phosphonated blocks was strongly influenced by the formation of anhydride links through reversible self-condensation reactions at elevated temperatures. Studies of thin copolymer films by tapping mode atomic force microscopy revealed nanophase-separated morphologies with continuous phosphonated domains. In addition, the acidic block copolymers were found to self-assemble into spherical micellar nanoparticles which, in turn, formed branched arrays of supramolecular "necklace-like" chain structures. Block copolymers equilibrated at 25 °C and 98% relative humidity reached proton conductivities in the order of 30 mS/cm at 130 °C.

Introduction

Polymers and copolymers containing vinylphosphonic acid and its ester derivatives have attracted an interest for a variety of different applications including materials for implants and tissue engineering,[1,2] dental cements,[3,4] flame-retardants,[5,6] and fuel cell membranes.[7−9] In particular, proton-exchange membrane fuel cells (PEMFCs) currently draw a tremendous attention because of their potential to achieve higher efficiencies than current power sources at a lower environmental impact.[10] The proton-exchange membranes in the PEMFC are today typically based on hydrated sulfonated polymers and serve to separate the electrodes and to efficiently facilitate the transport of protons from the anode to the cathode during fuel cell operation. It is currently a significant challenge to find viable alternatives to the perfluorosulfonated Nafion membrane, which starts to lose its water and conductivity at temperatures above 90 °C or at low relative humidities, thus severely limiting the applicability of the PEMFC.[11−13]

Polymers functionalized with alternative protogenic groups, including phosphonic acids[7−9] and different heterocycles,[14−18] have been investigated with the aim to overcome the shortcomings of the Nafion membrane. Recent results on phosphonated polymers have shown that high intrinsic proton conductivities may be reached provided that the local concentration of phosphonic acid groups is very high.[19] Moreover, the lower acidity of phosphonic acids, in relation to sulfonic acids, means that higher ionic contents are also necessary to attain high conductivities under hydrated conditions. In this context, poly(vinylphosphonic acid) (PVPA) has emerged as an interesting candidate because of its extremely high concentration of phosphonic acid which is directly attached to a flexible polymer chain. In contrast to, e.g., poly(*m*-phenylenephosphonic acid),[20] PVPA behaves like a monoprotic acid in water.[9] This is presumably because the proximity of the acid units in PVPA only allows the dissociation of one proton for electrostatic reasons. Furthermore, PVPA is water-soluble and shows a pronounced polyelectrolyte behavior in solution. In order to be used for membranes in contact with water, PVPA needs to be immobilized via, e.g., cross-linking or the formation of suitable copolymers with stable morphologies where the high phosphonic acid concentration is retained.

Block and graft copolymers in which ionic functions are concentrated to specific polymeric segments are interesting because of the characteristic self-assembly that occurs as a result of the thermodynamic incompatibility between the ionic and nonionic polymer segments.[21,22] The self-assembly typically leads to a variety of different morphologies that contain nanostructured ion conducting phases. Several investigators have reported on the impact of ordered and oriented ionic nanostructures on the properties of proton conducting membranes.[21] Ding et al.[23,24] have for instance reported a significantly higher conductivity in membranes based on unsulfonated polystyrene (PS) grafted with sulfonated PS in relation to membranes based on randomly sulfonated PS with similar ionic content. They attributed the high conductivity of the former membranes to the presence of an ordered ionic nanostructure in the graft copolymer membranes where the ionic groups were concentrated to form channels for efficient proton transport. There are still only very few papers on the morphologies and the proton conducing properties of phosphonated block copolymers.[25,26]

The interest in polymers containing vinylphosphonic acid has resulted in a number of recent reports on the polymerizability of vinylphosphonic acid and its derivatives.[27−29] The majority of the work has focused on radical polymerizations, and there are only a very limited number of reports on the anionic polymerization of dialkylvinyl phosphonates.[30,31] Yet, Gopalkrishnan[32] has

*Corresponding author: e-mail patric.jannasch@polymat.lth.se, Fax +46-46-222 4012.

 Published on Web 06/05/2009

reported the anionic polymerization of diethyl vinylphosphonate (DEVP) under classical conditions through initiation by butyllithium in THF at −78 °C. In addition, we have previously successfully grafted DEVP from 1,1-diphenylalkyl anions tethered to polysulfones.[9] Subsequently, polysulfones grafted with PVPA were produced by quantitative cleavage of the ester functions of the poly(diethyl vinylphosphonate) (PDEVP) grafts. The resulting copolymers were nanophase separated and showed high proton conductivities. These findings prompted us to also investigate block copolymers with PVPA segments. In the present work we have prepared and studied PS−PVPA diblock copolymers as model ionomers in order to investigate their nanostructures and properties as polymer electrolytes. The copolymers were prepared through sequential anionic polymerizations involving DEVP. To the best of our knowledge, this is the first report on the preparation of PVPA block copolymers and the use DEVP in sequential anionic polymerizations.

Experimental Section

Materials. Styrene (Aldrich; ≥99%) was dried for at least 24 h over CaH_2, then distilled under reduced pressure at 30 °C, and stored under argon. Tetrahydrofuran (THF, Merck, p.a.; >99.8%) was dried over molecular sieves (Acrôs; 4 Å, 8−12 mesh) during at least 24 h. The sieves were activated at 250 °C for 48 h under air and subsequently cooled to room temperature under vacuum. Diethylvinyl phosphonate (DEVP, Fluka; ≥97%) and 1,1-diphenylethylene (DPE, Aldrich; 99%) were used as received. A 2.5 M solution of *n*-butyllithium in hexanes (*n*-BuLi; Acrôs) was used as received after titration to determine the *n*-BuLi concentration.[33] Methanol (Prolabo; 99.9%), chloroform (Merk; p.a.; >99%), methylene chloride (Prolabo; HPLC; >99.8%), diethyl ether (Prolabo; Ph.Eur), *N*-methyl-2-pyrrolidinone (NMP, Acrôs Organics; 99%), and aqueous HCl (Normapur; p.a.; 37%) were used as received.

Preparation of PS−PDEVP Block Copolymers. The copolymer synthesis was carried out according to Scheme 1. A predried 250 mL round-bottomed glass reactor was equipped with a gas inlet and outlet, a thermometer, a septum, and a magnetic stirrer. In a typical procedure, the reactor was filled with 100 mL of dried THF and cooled down to −75 °C using a mixture of dry ice in isopropanol. The system was purged by argon at least seven times and left under a pressure of argon. Using a carefully dried syringe, small predetermined volumes of *n*-BuLi was first added to consume the small quantities of remaining impurities in the THF. Next, a specific amount of *n*-BuLi was added to act as initiator for the polymerization. The styrene was then slowly added dropwise (~0.1 mL/min) in order to keep the temperature below −70 °C. A yellow-orange color appeared immediately after adding the monomer, and the polymerization proceeded under stirring for 30 min. At the end of this period, a small aliquot of the reaction mixture was extracted and quenched in methanol in order to determine the molecular weight of the PS block. An amount of DPE was then injected at a ratio of *n*-BuLi:DPE equal to 1:1.2, resulting in an immediate red coloration of the reaction mixture. Next, DEVP was added dropwise, slow enough to keep the temperature below −65 °C. The reaction mixture was then colored in light yellow and was kept at −70 °C for 1.5 h before allowing it to heat up to room temperature. A small volume of methanol was finally injected to quench the polymerization after 2 h. The reaction mixture was then poured into methanol to isolate the copolymer. After drying the block copolymer under vacuum at 50 °C, the purity was checked by ^{1}H NMR spectroscopy. The yield of the polymerization of DEVP was calculated by comparing the weight of PDEVP in the copolymer and the weight of the monomers charged to the reactor. The weight of PDEVP in the copolymer was determined by weighting the dry copolymer and determining its PDEVP content by ^{1}H NMR spectroscopy.

Preparation of PS−PVPA Block Copolymers. The phosphonate esters of the PDEVP blocks were hydrolyzed to form PVPA blocks. An amount of diblock copolymer (~1 g) was dissolved in a minimum volume of dichloromethane. This solution was mixed with at least 100 mL of fuming hydrochloric acid and kept at reflux for at least 7 days. Then the polymer product was recovered by evaporating the liquid components using a rotary evaporator. The product was then dissolved in a minimum amount of THF and extracted with diethyl ether. The polymer was isolated after collecting the THF phase and evaporating the solvent. ^{1}H and ^{31}P NMR spectroscopy were used to verify the complete hydrolysis. The diblock copolymers in the ester and acid forms were designated as PS_x-*b*-$PDEVP_y$ and PS_x-*b*-$PVPA_y$, respectively, where x and y are the number-average degree of polymerization of the respective blocks. The theoretical ion-exchange capacity (IEC) of the acidic copolymers was calculated as the number of mmol of $-PO_3H_2$ units per g dry sample, thus taking into account only one of the two protons of the phosphonic acid group.[9]

Copolymer Characterization. Nuclear magnetic resonance (NMR) spectra were recorded using a Bruker Ultrashield Plus 400 MHz instrument. ^{1}H, ^{13}C, and ^{31}P NMR spectra were recorded at 400.13, 100.62, and 161.97 MHz, respectively. The chemical shifts (δ) were calibrated using the residual signal from the deuterated solvents $CDCl_3$ ($\delta = 7.27$ and 77 ppm for ^{1}H and ^{13}C NMR, respectively) or DMSO-d_6 ($\delta = 2.50$ and 39.7 ppm for ^{1}H and ^{13}C NMR, respectively).

Size exclusion chromatography (SEC) measurements were carried out to determine the number-average molecular weight (M_n) and polydispersity (M_w/M_n) of the PS blocks. The setup included three Shodex columns (KF-805, -804, and -802.5) in series and a Viscotek dual detector model 250. All samples were run at room temperature in chloroform at an elution rate of 1 mL/min. Calibration was performed by using PS standard samples from Polymer Laboratories, Ltd.

The thermal stability of the different copolymers was evaluated by thermogravimetric analysis (TGA) on a Q500 analyzer from TA Instruments. The data were collected from 100 to 600 °C after the samples were kept at 120 °C for 20 min. The samples were analyzed both under a nitrogen atmosphere at a heating rate of 10 °C/min and under air at a heating rate of 1 °C/min. Differential scanning calorimetry (DSC) measurements were carried out with a Q1000 instrument from TA Instruments. Samples were transferred to a hermetic pan that was sealed. The samples were then analyzed during the following sequence of cooling and heating scans: 0 °C → 150 → 0 → 200 → 0 → 250 → 0 → 300 °C. The cooling and heating rates were 40 and 20 °C/min, respectively, and the glass transition temperatures (T_g's) were evaluated from the data recorded during heating by identifying the inflection points.

Block copolymer morphologies were investigated by analyzing surfaces of thin films using atomic force microscopy (AFM). The block copolymers in the ester form were first dissolved in THF (ester form) or NMP (acid form) to a concentration of 10 mg/mL. All samples were then further diluted 100 times with THF and cast on freshly cleaved mica surfaces. The samples with highest molecular weight (PS_{337}-*b*-$PDEVP_{139}$ and PS_{337}-*b*-$PVPA_{139}$) were diluted to 60 μg/mL before casting. The copolymer surfaces were analyzed under ambient air using a Veeco's MultiMode V AFM in tapping mode. Simultaneous topographic and phase imaging was carried out at a scanning frequency of 0.5 Hz. The probe was TESP-SS (Super Sharp: 42 N/m, 320 kHz, 2−5 nm ROC, no coating). No image processing except flattening was done.

Water uptake measurements were made by first drying the PS−PVPA block copolymer samples to obtain their dry weights (W_{dry}) before transfer to a desiccator in which the relative humidity (RH) was kept at 98% by a saturated solution of $CuSO_4$. After equilibration, the weight of the swollen sample (W_{wet}) was measured and the water uptake (W_{water}) was calculated as $W_{water} = [(W_{wet} - W_{dry})/W_{dry}] \times 100\%$.

Scheme 1. Synthetic Pathway to PS−PVPA Diblock Copolymers by Sequential Anionic Copolymerization of Styrene and DEVP, Followed by Hydrolysis of the PDEVP Block

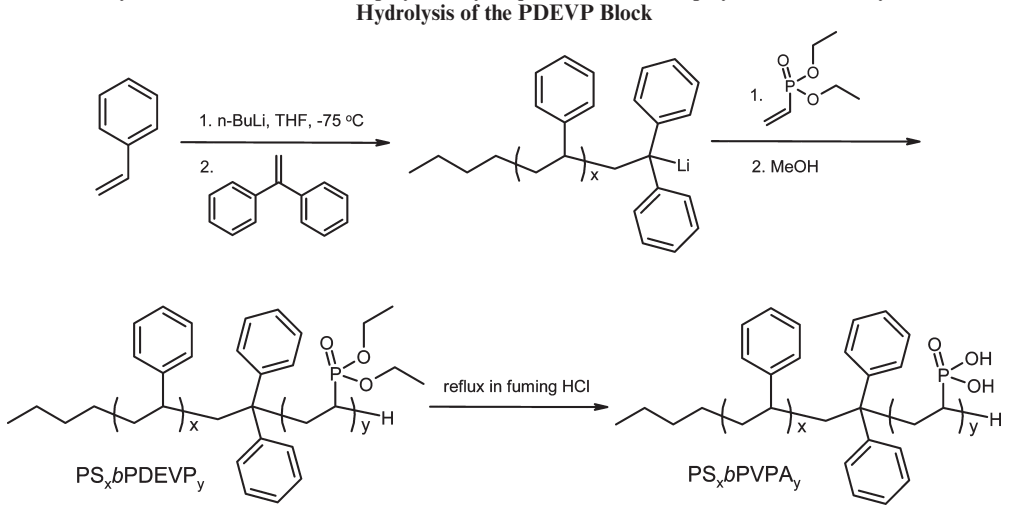

Scheme 2. Nucleophilic Attack by the Polystyryl Anion on the Phosphorus Atom of DEVP

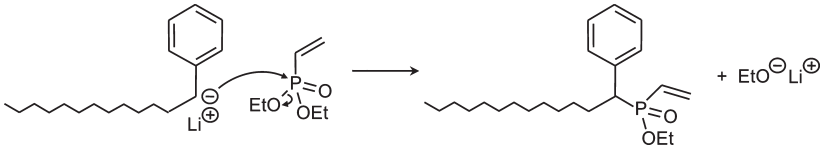

The proton conductivity was evaluated by electrochemical impedance spectroscopy (EIS) using a Novocontrol high-resolution dielectric analyzer V 1.01S equipped with a Novocool temperature system. Samples equilibrated at 98% RH were placed between two Au-plated electrodes separated by a flat PTFE ring with an inner diameter of 5 mm and a thickness of 250 μm to define the geometry of the cell. The conductivities of a Nafion115 membrane were measured in the plane of a membrane (8 × 8 mm) using two polished stainless electrodes after equilibrating the membrane at 100% RH at each temperature. Impedance data were gathered between −20 and 120 °C at increments of 10 °C over the frequency range of 10^{-1}−10^{7} Hz and a voltage amplitude of 50 mV. The data were subsequently analyzed using the software WinDeta from Novocontrol. The conductivity was determined by plotting the imaginary part of the conductivity versus the real part, and the conductivity was taken as the real value corresponding to the minimum imaginary response.

Results and Discussion

Block Copolymer Synthesis and Characterization. Previously it has been reported that high molecular weight PDEVP can be prepared by anionic polymerization directly from alkyllithium.[32] Encouraged by this result, we made initial attempts to polymerize DEVP directly from polystyryl anions at −78 °C in THF. However, these efforts were unsuccessful, and no polymeric product was obtained. We believe that the most probable reason was a side reaction involving an attack by the highly nucleophilic polystyryl anions on the phosphorus atoms of the DEVP monomer, as shown in Scheme 2. However, after adding a slight excess of DPE to the *n*-BuLi to form the less nucleophilic 1,1-diphenylhexyllithium it was possible to successfully initiate the polymerization of DEVP to fairly high molecular weights (> 30 000 g/mol). This is in line with the general reactivity of DPE[34] and also with our previous findings that it is possible to efficiently graft DEVP from 1,1-diphenylalkyllithium sites on polysulfones.[9] In the present work we have investigated sequential anionic polymerizations of styrene and DEVP to form PS−PVPA block copolymers after hydrolysis of the PDEVP block. To the best of our knowledge, this is the first report on the preparation of block copolymers via sequential anionic polymerization of DEVP.

Five diblock copolymers with different sizes of the PS and PVPA blocks were prepared by sequential anionic polymerizations according to Scheme 1. As seen in Table 1, the block copolymers contained between 30 and 70 wt % PVPA with block lengths between 5 and 15 kg/mol. In the first step, the polymerization of the styrene was initiated by *n*-BuLi. The molecular weights of the PS blocks were evaluated by SEC using PS standards and were in excellent agreement with the theoretical (targeted) values calculated from the charged amounts of *n*-BuLi and styrene. This demonstrated, as expected, that the styrene monomer was completely consumed and that the PS block length could be adequately controlled. The PS polydispersity ranged between 1.1 and 1.2. After adding an excess of DPE to the living polystyryl anions to form the less nucleophilic 1,1-diphenylalkyl anions, the DEVP was charged to successfully polymerize the second block.

A significant copolymer aggregation in organic solvents prevented a direct characterization of the PS−PDEVP block copolymers by SEC. Instead, the block copolymers were characterized indirectly by combining SEC data of the PS blocks and ^{1}H NMR data of the block copolymers. Representative ^{1}H and ^{31}P NMR spectra of PS-*b*-PDEVP are shown in parts a and b of Figure 1, respectively. The contents of the block copolymers were evaluated by comparing the integrated signal of the diethyl ester methylene protons of PDEVP at δ 4.1 with that of the PS phenyl protons between δ 6.25 and 7.25. Shifts from the diethyl ester methyl protons at δ 1.2, and shifts from the PS and PDEVP backbone methine and methylene protons between δ 0.9 and 2.75, were also observed in the spectra. The structure of the block copolymers was also confirmed by ^{13}C NMR results.[35] The ^{31}P NMR spectra showed a large signal corresponding

Table 1. Block Copolymer Synthesis and Molecular Structure Data

			DEVP content (wt %)		PS block[b]		PDEVP block[c]	PVPA block[c]	
acidic block copolymer	charged amounts $n_{BuLi}/n_{St}/n_{DEVP}$ (mmol/mmol/mmol)	DEVP yield (%)	^{1}H NMR	TGA[a]	M_n (kg/mol)	M_w/M_n	M_n (kg/mol)	M_n (kg/mol)	PVPA content (wt %)
PS_{34}-*b*-$PVPA_{50}$	0.40/13.5/20.7	97	68	70	3.5 (3.5)	1.2	8.2 (8.5)	5.4 (5.6)	61
PS_{34}-*b*-$PVPA_{71}$	0.40/13.5/32.5	86	77	77	3.5 (3.5)	1.2	11.7 (13.3)	7.7 (8.8)	69
PS_{68}-*b*-$PVPA_{69}$	0.20/13.5/13.0	100	62	62	7.1 (7.0)	1.1	11.4 (10.7)	7.5 (7.0)	51
PS_{102}-*b*-$PVPA_{55}$	0.21/20.0/9.6	100	41	46	10.6 (9.9)	1.1	9.0 (7.5)	5.9 (4.9)	36
PS_{337}-*b*-$PVPA_{139}$	0.12/40.0/17.7	97	42	39	35.0 (34.7)	1.1	22.8 (24.2)	15.0 (15.9)	30

[a] Determined via the weight loss associated with the degradation of the PS block during TGA analysis under nitrogen. [b] Determined by SEC using PS standards. Theoretical (targeted) values within parentheses. [c] Determined by combining SEC of the PS block and ^{1}H NMR results of the diblock copolymers. Theoretical values within parentheses.

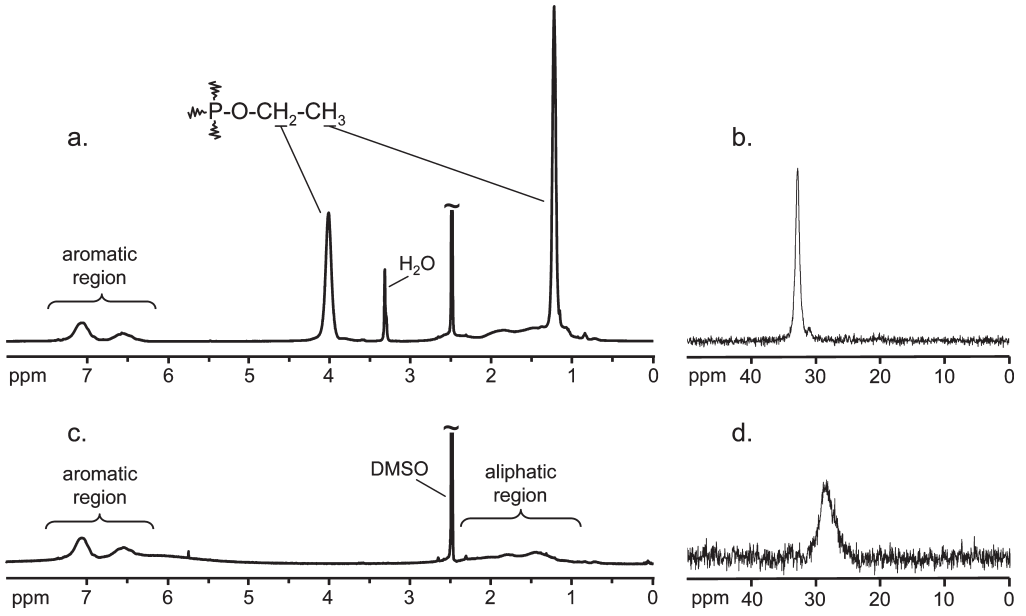

Figure 1. ^{1}H NMR (left) and ^{31}P NMR (right) spectra of block copolymers in the ester form (a, b) and in the acid form (c, d). The data were collected using sample PS_{34}-*b*-$PDEVP_{50}$ and PS_{34}-*b*-$PVPA_{50}$ in DMSO-d_6 solutions.

to the phosphorus of the PDEVP block at δ 32.8. The calculations to evaluate the PDEVP content showed that the control of the average M_n of the PDEVP block was fairly accurate, as seen in Table 1.

After characterization of the PS−PDEVP block copolymers, the latter block was transformed into PVPA through complete hydrolysis by reflux in aqueous HCl. Parts c and d of Figure 1 show typical ^{1}H and ^{31}P NMR spectra, respectively, of the PS−PVPA block copolymers. The quantitative hydrolysis of the PDEVP blocks was confirmed by the complete absence of the signals arising from the diethyl ester protons in the ^{1}H NMR spectra. Also, the broad band observed between δ 5.5 and 6.4 probably resulted from hydrogen-bonded phosphonic acid. In the ^{31}P NMR spectra, the shift of the diethyl ester derivative disappeared, and a broad band of the diacid appeared at δ 29.2. In some spectra, peaks originating from phosphonate anhydrides (P−O−P bridges) were observed at δ 21.

Thermal Stability. The thermal stabilities of the PS−PDEVP and PS−PVPA block copolymers were investigated by TGA both under N_2 and air atmosphere. Analysis under N_2 at 10 °C /min was performed to analyze the block copolymer contents. As shown in part a of Figure 2, the ester derivatives of the block copolymers degraded during three distinct steps. After the evaporation of small amounts of solvent residues from 200 °C, the first step at 300 °C corresponded to the loss of the diethyl ester groups via the formation of ethylene and phosphonic acid units.[36] The second step started at 400 °C and arose from the degradation of the PS block. The weight loss connected with this step was used to calculate the contents of the respective block copolymer. As seen in Table 1, the results in terms of PDEVP content agreed very well with the same content evaluated from NMR data. The third degradation step started at ~470 °C and indicated the breakdown of PVPA. The corresponding TGA traces of the acidic copolymers under nitrogen (Figure 2a) showed a gradual weight loss beginning at 150 °C. This corresponded to the loss of water formed in the self-condensation reactions of phosphonic acid, as shown in Scheme 3. Next followed the degradation of PS at ~400 °C, and then the PVPA degradation at 470 °C. Consequently, the degradation of the acid and ester derivatives of a given copolymer was very similar after reaching 350 °C under nitrogen.

Part b of Figure 2 shows the TGA traces of the acid derivatives recorded under air at 1 °C/min. This analysis was undertaken to evaluate the thermo-oxidative stability of the proton conducting polymers. The initial weight loss beginning at 110 °C increased with increasing content of PVPA and was connected to the condensation and loss of water (Scheme 3). The weight losses associated with the degradation steps under air were much less correlated to the PS content than the corresponding steps under nitrogen. Furthermore, under air a significant amount of carbonac-

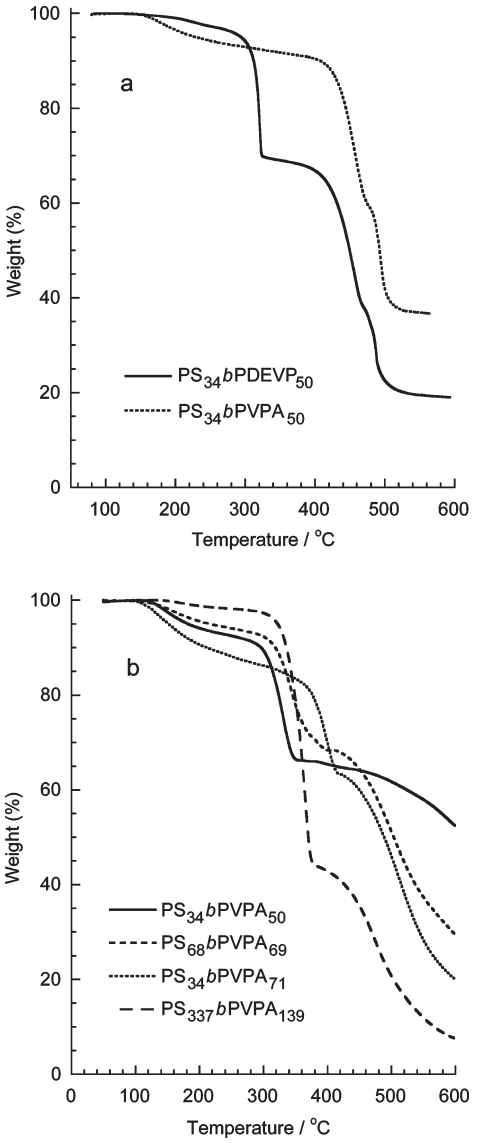

Figure 2. TGA traces of (a) block copolymer PS_{34}*b*$PDEVP_{50}$ (ester form) and PS_{34}*b*$PVPA_{50}$ (acid form) recorded at 10 °C/min under nitrogen and (b) TGA traces of the block copolymers in the acid form recorded at 1 °C/min under air.

Scheme 3. Formation of P−O−P Bonds through Intermolecular Self-Condensation Reactions of Phosphonic Acid Groups at Elevated Temperatures

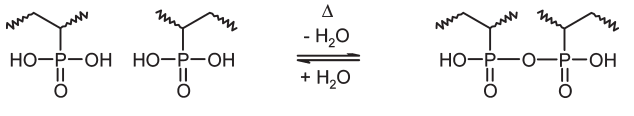

eous residues were left. The carbon formation is a known flame-retardation mechanism promoted by phosphoric acid.[37] The polymer degradation under air began between 300 and 370 °C depending on the copolymer. This was 30−100 °C below the corresponding degradation under nitrogen at 10 °C/min. Quite a similar difference between the degradation of PS under air and nitrogen has been reported at a heating rate of 10 °C/min.[38]

Glass Transitions. Completely amorphous diblock copolymers are normally phase separated and show two glass transitions arising from the phase domains formed by the two blocks.[21] If one of the blocks is ionic, there is usually a further phase separation on a much smaller scale between the polymer chains and the ionic groups which usually cluster together. The glass transitions of the present diblock copolymers were studied by DSC. The PS−PDEVP copolymers showed only one glass transition between 90 and 100 °C, followed by an irregular signal which may indicate some loss of material already below 130 °C.[39] Figure 3 shows the heating traces of PS_{337}*b*$PVPA_{139}$ from a sequence of heating and cooling scans where the sample was heated at progressively higher temperatures (see Experimental Section). The trace of the as-cast sample displayed a broad transition in the interval 50−100 °C when heated to 150 °C, which may indicate weakly segregated phase domains. After this first heating scan, two clear and separated glass transitions emerged at 100 and 180 °C during heating to 200 °C, which corresponded to the T_g's of the PS and PVPA phases, respectively. This confirmed that the PS and PVPA blocks were distinctly phase separated. During the third heating scan to 250 °C, the T_g's were shifted to 105 and 218 °C, respectively, and after the fourth heating scan to 300 °C the T_g's where found at 110 and 260 °C, respectively.

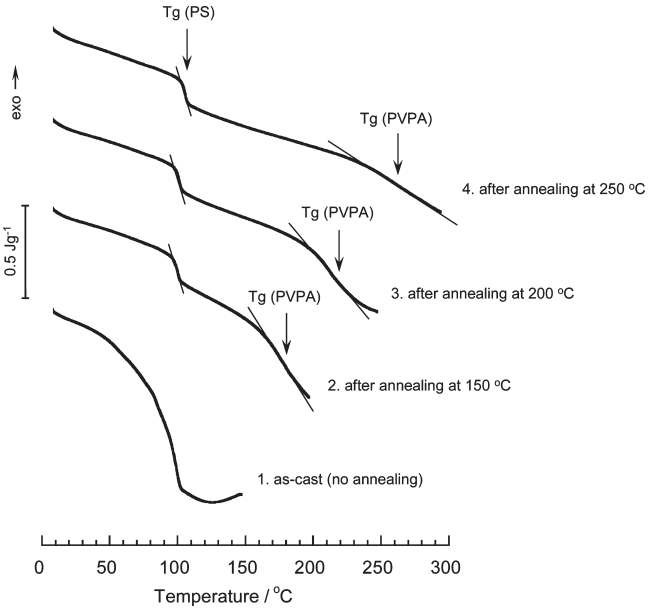

Figure 3. DSC heating traces of block copolymer PS_{337}*b*$PVPA_{139}$ showing the successively increasing T_g of the PVPA phase during the scan sequence: 0 °C → 150 → 0 → 200 → 0 → 250 → 0 → 300 °C at 10 °C/min.

The condensation reactions in the PVPA phase produced water at high temperatures, as shown by TGA. However, the condensation reactions also led to the formation of phosphonic anhydride bridges (P−O−P bonds) which reversibly cross-linked the PVPA chains and restricted their segmental mobility. Consequently, the T_g of the PVPA phase was found to increase with increasing annealing temperature because of the increasing concentration of cross-linking P−O−P bonds (Scheme 3). Similar observations have previously been made with polysulfones grafted with PVPA side chains (PSU*g*PVPA).[9] It can be envisaged that the condensation reactions, and thus the increase of the T_g of the PVPA blocks, proceeded with time during the annealing as long as the segmental mobility was sufficient. As the T_g approached the annealing temperature, the reactions slowed down, and consequently the onset of the glass transition finally ended up close to the annealing temperature. The data indicated that the condensation reaction rate was quite fast at temperatures above 150 °C. As seen in Figure 3, the effect on the

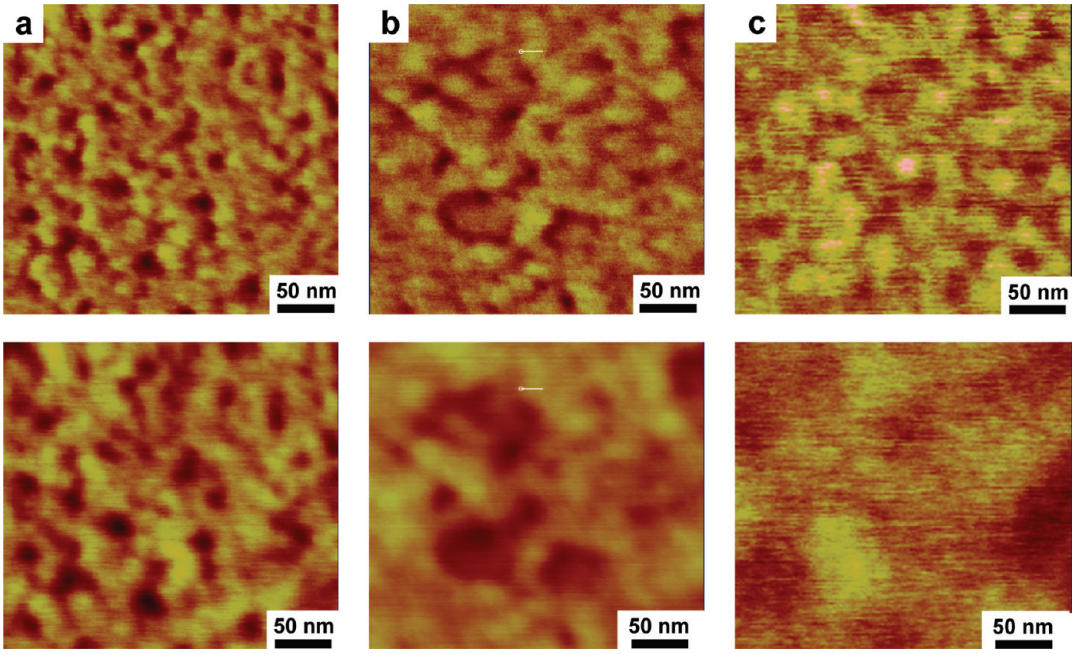

Figure 4. AFM tapping mode phase (upper) and topography (lower) images of thin films of diblock copolymers in the ester form: (a) PS_{34}*b*$PDEVP_{71}$, (b) PS_{68}*b*$PDEVP_{69}$, and (c) PS_{337}*b*$PDEVP_{139}$.

T_g by the annealing temperature decreased with increasing annealing temperature during the DSC experiment. This may be explained by increasing restrictions on the mobility of the phosphonic acid groups and thus slower kinetics of the condensation reactions as the concentration of anhydride bridges successively increased. The T_g of the PS phase also increased to some extent with increasing annealing temperature, which suggested that the segmental mobility of the PS blocks was influenced by the increasing restrictions of the PVPA blocks.

Block Copolymer Morphologies. Thin films of the block copolymers were cast on top of mica and analyzed by tapping mode AFM to study the morphology. Figure 4 shows the phase and topography images of the nonionic PS−PDEVP block copolymers. As seen, the images display structures with light and dark regions, corresponding the PS and PDEVP phases formed by the respective blocks. The thin films showed nanophase separated morphologies that seemed quite vague and irregular, indicating weak segregation and a high degree of phase mixing between the blocks. The phase images gave in most cases a more detailed account of the separation of the blocks than the topographic images.

The AFM images of the ionic PS−PVPA block copolymer films are shown in Figure 5. The images demonstrated clearly that these block copolymers self-assembled into phase-separated morphologies on the nanometer level. The phases appeared to be more distinctly segregated than the corresponding nonionic ester derivatives, with the dark regions representing the proton conducting PVPA domains and the bright regions representing the hydrophobic PS domains in phase images. Figure 5b shows the morphology of the film formed by the almost symmetrical block copolymer PS_{68}*b*$PVPA_{69}$ which displayed the sharpest phase separation typical of a lamellar-like structure. The clear segregation between the PS and PVPA blocks may be explained by the ionic and strongly hydrogen-bonding character of the PVPA block in combination with the hydrophobic character of PS block. Evaluated from the topographical images, the size of the PS domains were found to be in the intervals 5−10, 15−25, and 25−60 nm for the samples PS_{34}*b*$PVPA_{71}$, PS_{68}*b*$PVPA_{69}$, and PS_{337}*b*$PVPA_{139}$, respectively. The corresponding sizes of the PVPA domains were in the range 5−10, 10−20, and 10−15 nm, respectively. In all cases the block copolymers seemed to form morphologies with continuous proton conducting PVPA network structures. Although the blocks were distinctly segregated, the block copolymers displayed rather irregular morphologies. The formation of irregular nonperiodic cocontinuous morphologies in ionic block copolymer films has been reported to be beneficial over, e.g., periodic lamellar morphologies where the domains often orient parallel to the film surface and thus perpendicular to the direction of proton transport.[40] The reason for the formation of the irregular morphologies in the present case may arise from restrictions in molecular mobility in the self-assembly process of the block copolymers during the film formation. It has been argued that extensive hydrogen-bonded aggregates of phosphonic acids exist even in aqueous solutions.[41] In addition, as already mentioned above, the presence of reversible intermolecular anhydride bridges may further restrict the mobility. In studies of sulfonated diblock copolymers, several investigators have observed that the morphology was well-ordered for diblock copolymers having a partially sulfonated block with a low ionic content, while the corresponding diblock copolymers having a fully sulfonated block with a high ionic content displayed more disordered structures.[40,42] Because of the high concentration of phosphonic acid in the PVPA block, the present block copolymers are likely to fall in the latter category.

In addition to nanostructured films, the amphiphilic block copolymers were also found to self-assemble to build micellar aggregates in the form of particles, as seen in the AFM images shown in Figure 6. The spherical aggregates in turn arranged themselves into arrays to form branched "necklace-like" chain structures. The micellar aggregates of copolymer PS_{34}*b*$PVPA_{71}$, shown in Figure 6, had diameters within the range 30−50 nm and heights of 18−20 nm when imaged by AFM after being deposited on mica surfaces from dilute NMP solutions. The explanation for the formation of the nanoparticle networks might be connected to a "stickiness" of the micellar aggregates because of the strong hydrogen

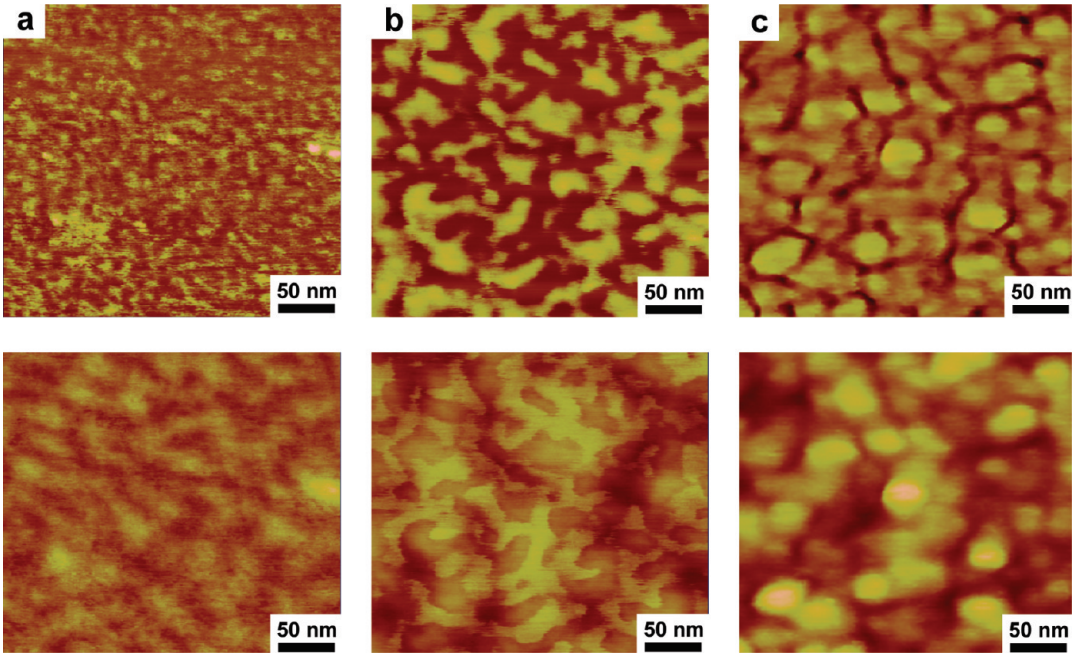

Figure 5. AFM tapping mode phase (upper) and topography (lower) images of thin films of diblock copolymers in the acid form: (a) $PS_{34}bPVPA_{71}$, (b) $PS_{68}bPVPA_{69}$, and (c) $PS_{337}bPVPA_{139}$.

Scheme 4. Proposed Mechanism for the Formation of the Block Copolymer Films from Micellar Aggregates with PS Cores (Yellow) and PVPA Coronas (Brown)

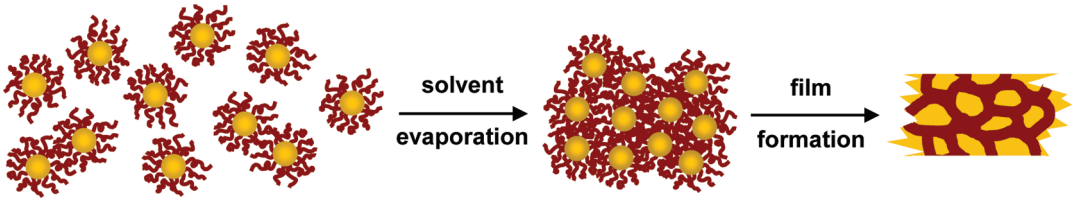

bonding or anhydride formation between the phosphonic acid groups. The same kinds of "supermicellar" structures have previously been reported for carboxylic acid functional block copolymers in aqueous medium.[43] The present highly amphiphilic block copolymers most probably formed the micellar aggregates with PS cores and PVPA coronas already in solution. We believe that the films were then formed according to the mechanism shown in Scheme 4, where the aggregates first associated during solvent evaporation and then collapsed during the final stage during which the PS cores were deformed. The mechanism is consistent with the observation of continuous proton conducting PVPA network domains in all the AFM images. This is perhaps most clearly seen for copolymer $PS_{337}bPVPA_{139}$ in Figure 5c.

Acid-functionalized particles have previously been prepared and studied for use as fuel cell membrane materials. Holdcroft et al.[44,45] have investigated films formed by latex nanoparticles with surfaces functionalized with sulfonic acid. Films with continuous ionic channels for proton conduction formed naturally when annealing close-packed particles. In fact, the morphology of these films resembled that seen for $PS_{337}bPVPA_{139}$ in Figure 5c, indicating a similar film formation mechanism. However, the present copolymer film showed phase separation on a smaller scale (25−60 nm) as compared to the latex films (~80 nm) and contained a larger fraction of ionic phase. Very recently, micellar structures of phosphorus-containing block copolymers have been used as templates to control the size and shape of gold nanostructures.[46]

Table 2. Membrane Properties of the Block Copolymers

block copolymer	theoretical IEC (mmol/g)	$T_{d,5\%}$[a] (°C)	w_{water}[b] (%)	$[H_2O]/[-PO_3H_2]$[b]
$PS_{34}bPVPA_{50}$	5.6	305	137	13
$PS_{34}bPVPA_{71}$	6.4	370	146	13
$PS_{68}bPVPA_{69}$	4.8	320	137	16
$PS_{337}bPVPA_{139}$	2.8	330	20	4

[a] Temperature for the detection of 5% weight loss when heated under air at 1 °C/min. [b] Measured after equilibration at 98% RH and 25 °C.

Water Uptake and Proton Conductivity. The uptake of water is a fundamentally important property of proton conducting polymers and determines to a great extent the level of conductivity. Generally, phosphonated polymers absorb less water molecules per acid group than the corresponding sulfonated polymers.[30,31] Yet, the high IEC values of the present block copolymers still led to high levels of water uptake, as seen in Table 2. The water uptake at 98% RH and 25 °C seemingly depended on both the PVPA content and the molecular weight of the PS block. Thus, copolymer $PS_{337}bPVPA_{139}$ had a quite low water uptake of 20 wt %, while copolymer $PS_{34}bPVPA_{71}$ took up 146 wt % water. The water uptake corresponded to $\lambda = 4-16$ water molecules absorbed per phosphonic acid unit. In comparison, a PSU*g*PVPA containing 57 wt % PVPA (IEC = 5.3 mmol/g, $M_{n(PVPA)} = 5.8$ kg/mol) absorbed 125 wt % water at 100% RH (20 °C),[9] while $PS_{34}bPVPA_{50}$ (61 wt % PVPA, IEC = 5.6 mmol/g, $M_{n(PVPA)} = 5.4$ kg/mol)

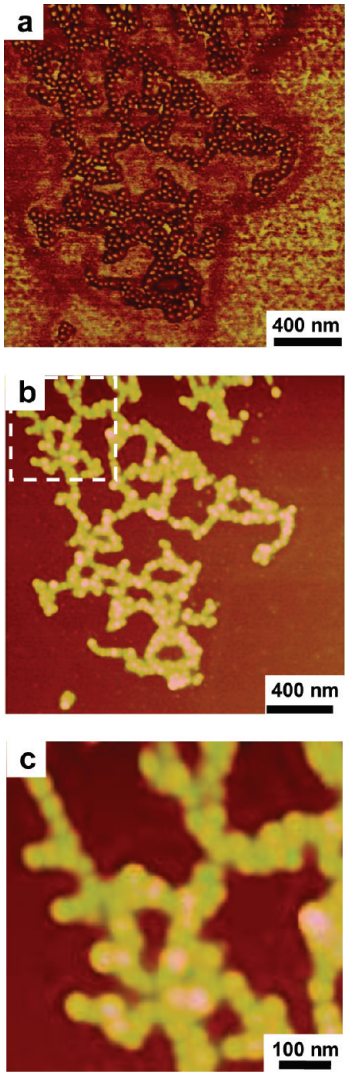

Figure 6. AFM tapping mode phase (a) and topography (b) images of spherical block copolymer $PS_{34}bPVPA_{71}$ aggregates showing their self-assembly into linear "necklace-like" chain structures. Image (c) shows a magnification of the framed section of image (b).

absorbed 137 wt % water at 98% RH (25 °C). Because of the still very limited number of investigations of phosphonated polymers as fuel cell materials, it is difficult to find relevant data from other research groups for comparison. Subianto et al.[25] have reported a water uptake of close to 100 wt % for phosphonated poly(styrene-*b*-[ethylene-*co*-butylene]-*b*-styrene) (SEBS) triblock copolymers (IEC = 0.7 mmol/g) at 40 °C and 100% RH. The high water uptake in relation to the IEC value may result from the soft rubbery hydrophobic phase ($T_g = -40$ °C), in relation to the glassy PS phase ($T_g \approx 100$ °C) of the present diblock copolymers, which allows a higher degree of deformation during swelling. Kaltbeitzel et al.[47] have previously measured a water uptake of 85 wt % at 98% RH at 24 °C for a linear homo-PVPA sample with a molecular weight of 62 kg/mol prepared by radical polymerization.

The proton conductivity of the three copolymers with the highest IEC was measured by EIS in a sealed cell after equilibration at 98% RH and 25 °C. The results are shown in Figure 7 together with the corresponding data of Nafion 115. As seen, the conductivity of the block copolymers increased sharply with the temperature below 0 °C as a result of the melting of the absorbed water. After 0 °C the conductivity increased moderately to reach ~30 mS/cm at

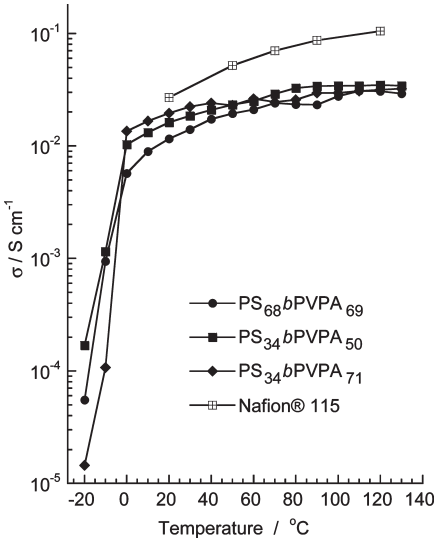

Figure 7. Conductivity data of PS−PVPA block copolymers measured by EIS in a sealed cell after equilibration at 98% RH and 25 °C.

130 °C, which may be compared to >100 mS/cm reached by Nafion 115 under the same conditions. Notably, all three block copolymers attained approximately the same level of conductivity at 130 °C, indicating a quite complex dependence on IEC, block lengths, and morphology. A more comprehensive study needs to be carried out to clarify these relationships. The PSU*g*PVPA containing 57 wt % PVPA (IEC = 5.3 mmol/g) reached a conductivity of 93 mS/cm under 100% RH at 130 °C.[9] Jin et al.[48] have very recently prepared porous silica nanoparticles functionalized with phosphonic acid by surfactant templated condensation of various alkoxysilanes. The high surface concentration of acid gave proton conductivities of 15 mS/cm at 130 °C and 100% RH. Subianto et al.[25] measured conductivities in the range of 2−4 mS/cm for the phosphonated SEBS triblock copolymers (IEC = 0.7 mmol/g) at room temperature and 100% RH. The higher conductivity values of the present block copolymers, between 10 and 20 mS/cm at 20 °C, may be explained by the higher IEC.

Conclusions

The current work has demonstrated the possibilities of using DEVP in sequential anionic polymerizations to prepare block copolymers. The control of the block sizes of the PS−PDEVP copolymers was satisfactory and might be improved by further optimizations of the synthesis procedure. The PDEVP blocks were readily and quantitatively transformed into PVPA blocks by hydrolysis under acid conditions. As expected, both the PS−PDEVP and PS−PVPA block copolymers formed nanostructured films. Self-assembly on two different levels most probably preceded the film formation of the latter copolymers; first macromolecular self-assembly to form the micellar nanoparticles, followed by self-association of the nanoparticles to form the "necklace"-like chain structures. The films had different morphologies depending of block copolymer composition and molecular weight, but all contained continuous network domains of proton conducting PVPA, consistent with the proposed film forming mechanism. Presumably because of the low molecular weights of the PS blocks and the nanostructure of the films, the block copolymers took up quite large amounts of water and reached comparatively high proton conductivities.

Acknowledgment. This work was funded by the Integrated Project AUTOBRANE under the 6th Framework Programme of

the European Commission. We thank Dr. Mark Ingratta for assistance with the carbon NMR measurements.

Supporting Information Available: ^{13}C NMR spectrum and DSC thermogram of PS−PDEVP block copolymers. This material is available free of charge via the Internet at http://pubs.acs.org.

References and Notes

(1) Tan, J.; Gemeinhart, R. A.; Ma, M.; Saltzman, W. M. *Biomaterials* **2005**, *26*, 3663–3671.
(2) Gemeinhart, R. A.; Bare, C. M.; Haasch, R. T.; Gemeinhart, E. J. *J. Biomed. Mater. Res. A* **2006**, *78A*, 433–440.
(3) Ellis, J.; Anstice, M.; Wilson, A. D. *Clin. Mater.* **1991**, *7*, 341–346.
(4) Adusei, G. O.; Deb, S.; Nicholson, J. W. *Dent. Mater.* **2005**, *21*, 491–497.
(5) Banks, M.; Ebdon, J. R.; Johnson, M. *Polymer* **1994**, *35*, 3470.
(6) Jiang, D. D.; Yao, Q.; McKinney, M. A.; Wilkie, C. A. *Polym. Degrad. Stab.* **1999**, *63*, 423–434.
(7) Gubler, L.; Kramer, D.; Belack, J.; Unsal, O. *J. Electrochem. Soc.* **2007**, *154*, B981.
(8) Steininger, H.; Schuster, M.; Kreuer, K. D.; Kaltbeitzel, A.; Bingol, B.; Meyer, W. H.; Schauff, S.; Brunklaus, G.; Maier, J.; Spiess, H. W. *Phys. Chem. Chem. Phys.* **2007**, *9*, 1764.
(9) Parvole, J.; Jannasch, P. *Macromolecules* **2008**, *41*, 3893.
(10) de Bruijn, F. *Green Chem.* **2005**, *7*, 132.
(11) Zhang, J.; Xie, Z.; Tang, Y.; Song, C.; Navessin, T.; Shi, Z.; Song, D.; Wang, H.; Wilkinson, D. P.; Liu, Z.-S.; Holdcroft, S. *J. Power Sources* **2006**, *160*, 872.
(12) Roziere, J.; Jones, D. J. *Annu. Rev. Mater. Res.* **2003**, *33*, 503.
(13) Maier, G.; Meier-Haack, J. *Adv. Polym. Sci.* **2008**, *216*, 1.
(14) Herz, H. G.; Kreuer, K. D.; Maier, J.; Scharfenberger, G.; Schuster, M. F. H.; Meyer, W. H. *Electrochim. Acta* **2003**, *48*, 2165.
(15) Schuster, M. F. H.; Meyer, W. H.; Schuster, M.; Kreuer, K. D. *Chem. Mater.* **2004**, *16*, 329.
(16) Granados-Focil, S.; Woudenberg, R. C.; Yavuzcetin, O.; Tuominen, M. T.; Coughlin, E. B. *Macromolecules* **2007**, *40*, 8708.
(17) Persson, J. C.; Jannasch, P. *Macromolecules* **2005**, *38*, 3283.
(18) Persson, J. C.; Jannasch, P. *Chem. Mater.* **2006**, *18*, 3096.
(19) Schuster, M.; Rager, T.; Noda, A.; Kreuer, K. D.; Maier, J. *Fuel Cells* **2005**, *5*, 355.
(20) Rager, T.; Schuster, M.; Steininger, H.; Kreuer, K. D. *Adv. Mater.* **2007**, *19*, 3317.
(21) Yang, Y. S.; Siu, A.; Peckham, T. J.; Holdcroft, S. *Adv. Polym. Sci.* **2008**, *215*, 55.
(22) Smart, T.; Lomas, H.; Massignani, M.; Flores-Merino, M. V.; Perez, L. R.; Battaglia *Nano Today* **2008**, *3*, 38.
(23) Ding, J. F.; Chuy, C.; Holdcroft, S. *Macromolecules* **2002**, *35*, 1348.
(24) Ding, J. F.; Chuy, C.; Holdcroft, S. *Chem. Mater.* **2001**, *13*, 2231.
(25) Subianto, S.; Choudhury, N. R.; Dutta, N. K. *J. Polym. Sci., Polym. Chem.* **2008**, *46*, 5431.
(26) Cho, C. G.; Kim, S. H.; Park, Y. C.; Kim, H.; Park, J. W. *J. Membr. Sci.* **2008**, *308*, 96.
(27) Bingol, B.; Hart-Smith, G.; Barner-Kowollik, C.; Wegner, G. *Macromolecules* **2008**, *41*, 1634.
(28) Komber, H.; Steinert, V.; Voit, B. *Macromolecules* **2008**, *41*, 2119.
(29) David, G.; Boyer, C.; Tayouo, R.; Seabrook, S.; Ameduri, B.; Boutevin, B.; Woodward, G.; Destarac, M. *Macromol. Chem. Phys.* **2008**, *209*, 75.
(30) Lafitte, B.; Jannasch, P. *Adv. Fuel Cells* **2007**, *1*, 119.
(31) Rusanov, A. L.; Kostoglodov, P. V.; Abadie, M. J. M.; Voytekunas, V. Y.; Likhachev, D. Y. *Adv. Polym. Sci.* **2008**, *216*, 125.
(32) Gopalkrishnan, S. Ph.D. Thesis, Rutgers the State University of New Jersey, New Brunswick, **1988**.
(33) Burchat, A. F.; Chong, J. M.; Nielsen, N. *J. Organomet. Chem.* **1997**, *542*, 281.
(34) Quirk, R. P.; Yoo, T.; Lee, Y.; Kim, J.; Lee, B. *Adv. Polym. Sci.* **2000**, *153*, 67.
(35) A typical ^{13}C NMR spectrum of a PS−PDEVP copolymer can be found as Supporting Information.
(36) Inagaki, N.; Goto, K.; Katsuura, K. *Polymer* **1975**, *16*, 641.
(37) *Plastics Flammability Handbook: Principles, Regulations, Testing, and Approval*; Troitzsch, J., Ed.; Hanser Publishers: Munich, 1983; Chapter 5.1.2.2.
(38) Peterson, J. D.; Vyazovkin, S.; Wight, C. A. *Macromol. Chem. Phys.* **2001**, *202*, 775.
(39) A typical DSC thermogram of a PS-PDEVP copolymer can be found as Supporting Information.
(40) Elabd, Y. A.; Napadensky, E.; Walker, C. W.; Winey, K. I. *Macromolecules* **2006**, *39*, 399.
(41) Kosolapoff, G. M. *J. Am. Chem. Soc.* **1952**, *74*, 3427.
(42) Rubatat, L.; Shi, Z. Q.; Diat, O.; Holdcroft, S.; Frisken, B. J. *Macromolecules* **2006**, *39*, 720.
(43) Abraham, S.; Ha, C. S.; Batt, C. A.; Kim, I. *J. Polym. Sci., Polym. Chem.* **2007**, *45*, 3570.
(44) Gao, J.; Lee, D.; Yang, Y. S.; Holdcroft, S.; Frisken, B. J. *Macromolecules* **2005**, *38*, 5854.
(45) Gao, J.; Yang, Y. S.; Lee, D.; Holdcroft, S.; Frisken, B. J. *Macromolecules* **2006**, *39*, 8060.
(46) Noonan, K. J. T.; Gillon, B. H.; Cappello, V.; Gates, D. P. *J. Am. Chem. Soc.* **2008**, *130*, 12876.
(47) Kaltbeitzel, A.; Schauff, S.; Steininger, H.; Bingol, B.; Brunklaus, G.; Meyer, W. H.; Spiess, H. W. *Solid State Ionics* **2007**, *178*, 469.
(48) Jin, Y. G.; Qiao, S. Z.; Xu, Z. P.; da Costa, J. C. D.; Lu, G. Q. *J. Phys. Chem. C* **2009**, *113*, 3157.